Effect of Aperture Averaging on a 570 Mbps 42 km Horizontal Path Optical Link

K. E. Wilson and A. Biswas
Jet Propulsion Laboratory California Institute of' Technology
S. Bloom and V. Chang
Thermo Trex Corp.

ABSTRACT

Optical communications offer high data rate satellite to ground communications in a small, low mass, and low power consumption package. However, hrrbulcncc-induced scintillation degrades the link performance as the zenith angle increases. To investigate the effect of atmospheric turbulence on the optical link at high zenith angles, wc performed a 570 Mbps optical communications link across a 42 km horizontal path, and have measured the effects of aperture averaging on the irradiance variance. The variance clearly showed a dependence on the aperture sire, decreasing with increasing aperture size. These results were used to calculate the log-amplitude variance and the atmospheric structure constant, C_n^2, across the link. The bit error rates across the link were also measured. The results show that the link performance was dominated by burst errors with error rates that ranged from 10^{-6} to 10^{-2}, increasing with decreasing aperture size.

1. 1NTRODUCTION

NASA's ncw Earth sensing satellites will require high rate communications to get their data down to the ground. Although rf communications is currently the baseline technology, optical communication is being considered a viable means of supplementing rf capabilities to meet the communications demand as industrial competitors vic for frequency allocations to support the expanding high resolution imagery, direct satellite broadcast, and global cellular communications markets. The demand is fierce and is expected to increase with public demand for ever increasing communications services.

Unlike rf communications, optical communication has no bandwidth allocation challenges; narrow line tunable lasers and atomic line filters of today's technology put such considerations far into the future. Propagation through the atmosphere is the challenge to optical communications, with cloud cover and beam scintillation the major causes of signal degradation. Site diversity, an approach in which receivers in the network arc situated in uncorrelated weather cells, mitigates the impact of cloud cover, and large aperture receivers can be used to reduce the effects of turbulence-induced scintillation. However, large receivers not only cost more but may be undesirable in certain applications such as on aircraft or unmanned airborne vehicles where size is an important consideration. A knowledge of the reduction in scintillation with increasing aperture is an important consideration in the design of these types of optical links.

Wc have measured the effects of aperture averaging on a 570 Mbps 42 km-long horizontal-path optical communications link between Strawberry Peak (height 1.85 km) and Table Mountain (height 2.2 km), two mountains in the Southern California San Bernadino and San Gabriel mountain chains, respectively. The results arc presented in this paper. The experiment and hardware arc described in Section 2 and the data and analysis in Section 3. Measurements were made at three intervals beginning at 12:00, 4:00 A.M. and 6:00 A.M. using apertures ranging from 4 cm to 29 cm. During the midnight run there were low clouds in the sky and wc measured a log-amplitude variance of 0.28. At 4:00 A.M. it was cold, windy and clear and wc measured a log-amplitude variance of 0.37. Measurements at 6:00 A.M. were made through thin haze and the measured Iog-amplitude variance was 0.27. Log-an iplitude variances in this range arc almost into the saturation region but arc still in the region of validity of the Rytov approximation to the wave equation.[1,2] Wc have analyzed our data assuming the Rytov approximation and a Kolmogorov turbulence spectrum in the inertial subrange.[3]

Measurements of the aperture averaging factor were consistent over the experiment durat ion and showed the expected decrease in variance with increasing aperture. The calculated refractive index structure constant, C_n^2, ranged from 7x10-17 to 9x10-^{17} over the duration of the experiment; and is in reasonable agreement with theoretical predictions of C_n^2 at these

elevations. [4] The bit error rates (BER) measured at midnight for the various aperture settings arc also given in Section 3. Measurements were made at onc second intervals over a ten to fifteen-second period, and the average BERs and standard deviations were determined for the interval. The data showed a distinct reduction in BER as the aperture size was increased, with a BER of approximately 2x10-6 measured for the 28.7 cm aperture. Conclusions arc given in Section 4, and the contributions and support of persons, not listed among the authors, but who nevertheless were instrumental in the success of this experiment arc acknowledged in Section 5.

2. EXPERIMENT DESCRIPTION

Laser transmission was from Strawberry Peak with reception at Table Mountai n, 42 kilometers away. Experiments were performed at three intervals between midnight and 6:00 A.M. Two sets of scintilla{ ion data (10,000 data points taken al a sampling interval of 0.2 seconds) were recorded for each aperture setting in each experimental run. Bit error rate measurements were taken at one-second intervals for 10 to 15 seconds.

The laser transmitter was a Spectra Diode Labs (SDL) 5421-G 1 single mode 150 mW semiconductor laser diode emitting at 811 nm, and mounted in a Rodenstock "Light Pen", A four-element lens set in the Light Pen reduced the beam divergence to 250 microradians, and a Rodenstock afocal cylindrical-lens-set circularized the beam to 7 mm diameter. To ensure adequate SNR at the receiver for the smaller receiver aperture sctt i rigs, a telescope was used to further reduce the laser beam divergence to approximately 80 microradians. The overall loss in the transmitter optical train was 5 dB with 47 mW of optical power propagated to the receiver.

The laser diode drive electronics consisted of a DC bias current combined with an AC modulation that generated a repeat ing bit pat tern at S70. 1 Mbit/sec. The amplified AC signal provided 100 mA peak-to-peak current swing above a 75 ma bias voltage. The current to the laser varied from about 25 mA ("O" or "low" bit) to 125 mA (" 1" or "high" bit), and a Broadband Communications Products Model 100 sequence generator was used to generate the pseudo-noise (PN) modulation sequence.

The receiving telescope was a 0.6-m astronomical telescope that stands approximately 8 meters above the ground. Looking towards the transmitter the terrain is relatively flat for about 70 meters after which it falls rapidly to the valley below. The telescope was operated in the coude mode. This allowed the effective receiving aperture to be adjusted by varying the size of the aperture positioned in front of the focusing lenses L 1 and L2. Sec figure 1. The loss in the receiver opt ical train was 9 dB; 7 dB from the telescope's central obscuration, and 2 dB from the five mirrors in the coude path. Wc measured 500 nanowatts of optical power at t hc coude focus for the fully opened telescope aperture. This corresponded to an overall link loss of 55 dB, of which 22 dB was duc to free space losses and 33 dB was duc to atmospheric attenuation.

Irradiance fades were measured using a low bandwidth United Detector Technologies (UDT) Model 10-D pin diode. A beamsplitter (BS) positioned between the lens-pair and the UDT detector reflected 40% of the beam to the APD, and allowed simultaneous measurement of the signal fades and the link bit error rate. Figure 2 shows the superposition of the APD and pin diode t races as displayed on the Tektronix DSA 602A oscilloscope. Thc at mosphcric scintillation, upper trace, is seen to track the high speed data stream detected by the APD.

A modified EG&G C30998-CD2036 APD (SLiK[TM] APD) with 359 MHz bandwidth performance was used as the high speed communications detector. The detector was biased to achieve high responsivity, 600 KV/W, at the operating wavelength and had a noise equivalent power of 0.02 pW/√H z at the bias voltage. The detector was terminated into the recommended AC coupled 500 Ω load, and excess electronic noise was minimized by mounting the detector very c1osc to the Elantec EL2072 buffer amplifier.

A Broadband Communications Products Model 50B bit synchronizer/clock recovery unit, and a Broadband Communications Products Model 200 sequence detector were used to make bit error rate measurements. A tapped register identical to that of the transmitter gave an error pulse when the incoming signal deviated from the expected pattern. The error pulses produced in the bit error rate tester (BERT) were counted using a Philips PM6666 counter/timer. The BERT displayed the number of errors detected over a onc second interval, and the results were averaged over the measurement interval for each aperture setting.

3. ANALYSIS AND EXPERIMENTAL RESULTS

3.1 Calculation of σ_x^2

The solution of the wave equation for propagation in a turbulent medium is given in terms of random variable analysis where means and variances define the wave propagation characteristics. For log-amplitude variances $\sigma_x^2 < 0.5$ the wave equation can be approximated by the Rytov solution to the scalar wave function [5] given by

$$U(r) = U_o(r)e^{(\chi+iS)}$$

Where $X = (\ln A/A_o)$ and S are the normalized log-amplitude and phase, respectively, and both X and S are normally distributed. Experimentally we measure the flux F over a collecting aperture of diameter D and determine the intensity $I (= 4F/\pi D^2 = UU^*)$, its mean $<UU^*>$ and its variance σ_I^2. These quantities are simply related to the log-amplitude variance σ_x^2, and the log-intensity variance $\sigma_{\ln I}^2$. A relationship that can be derived by starting with the mean intensity

$$<lx.?" >=< U_oU_o^* >< e^{2\chi} > \qquad 3.1$$

and using the properly of Gaussian random variables

$$< e^{ap} >= e^{(a<p>+0.5(a^2)<(p-<p>)^2>)}$$

This gives

$$< e^{2\chi} >= e^{2<\chi>+2<(\chi-<\chi>)^2>}$$

and

$$< U(r)U^*(r) >=< U_o(r)U_o^*(r) > e^{2(<\chi>+\sigma_\chi^2)}. \qquad 3.2$$

Atmospheric turbulence is non-d issapative and in the absence of absorption energy must be con.served. Then

$$<UU^* >=< U_oU_o^* >$$

i.e.,

$$<\chi>=-\sigma_\chi^2. \qquad 3.3$$

We measured the irradiance fluctuations through a collecting aperture of diameter D and calculate the normalized intensity variance σ_I^2/I_o given by:

$$\frac{\sigma_I^2}{I_o} = \left(\frac{< I^2 >}{I_o^2} - \frac{< I >^2}{I_o^2}\right). \qquad 3.4$$

Where $<I/I_O>^2 = 1$, and $<(I/I_O)^2> = exp(4\sigma_x^2)$, then

$$\frac{\sigma_I^2}{I_0} = e^{4\sigma_\chi^2} - 1, \qquad 3.5$$

and

$$\frac{\sigma_I^2}{I_0} = e^{\sigma_{\ln I}^2} - 1 \qquad 3.6$$

Typical histograms of the log intensity distribution for data taken with the 4 cm and 28 cm apertures along with the fit ted log-normal distribution is shown in figure 3. In general we obtained excellent agreement between the variances for the fit and measurement for the large apertures, but not as good agreement for the small apertures. Since in both cases 10,000 data points were taken, we believe that the discrepancy at the small aperture setting is caused by detector noise. Table 1 gives the normalized irradiance variances for the various apertures and experiment times.

Low signal-to-noise at the smaller apertures limited the minimum effective receiver aperture to 4 cm. We determined the log-amplitude variance by first determining the irradiance variance for a zero diameter receiver from the y intercept of the plot of σ_I^2/I_o vs. the Fresnel number $(kD^2/4L)^{1/2}$ and then using eqn. [3.5] to calculate 0_x^2. The plot is shown in figure 4 where $k = 2\pi/\lambda$ is the wave number for the optical wave, and L= 4?. km is the length of the propagation

path. Table 1 shows that the log-amplitude variance was 0.28 at midnight, 0.37 at 4:00 A.M. when it was cold and windy, and 0.27 at 6:00 A.M.

3.2 Determination of C_n^2

Local temperature and pressure fluctuations generate turbulence cells ranging from millimeters (inner scale l_0) to meters (outer scale L_0) that induce refractive index variations along the beam path. The refract ive index profile is defined by the structure constant $C_n^2(z)$, where z is defined in different models as either altitude relative to sca level or height above the ground It has been shown [6] that the log-amplitude variance in eqn. 13.5] can be expressed in terms of the turbulence spectrum as

$$\sigma_\chi^2 = \int_0^\infty 2\pi K \Phi_\chi(K) dK. \qquad 3.7$$

Where K is the spatial frequency, and $\Phi_x(K)$ is the log-amplitude Wiener spectrum. For a spherical wave propagating in a t urbulence spect rum that obeys the Kolmogorov law., the Weiner spectrum is given by

$$\Phi_\chi(K) = 2\pi(0.033K^{-11/3})k^2 \int_0^L C_n^2(z) \sin^2\left[\frac{K^2 L(L-z)}{2zk}\right] dz. \qquad 3.8$$

Substituting eqn. [3.8] in eqn. [3.7] wc get

$$\sigma_\chi^2 = 4\pi^2(0.033)k^2 \int_0^L C_n^2(z) dz \int_0^\infty \sin^2\left[\frac{K^2 L(L-z)}{2zk}\right] K^{-8/3} dK \qquad 3.9$$

Extending the range of integration in eqn. [3.9] from the inertial subrange $2\pi/L_0 < K < 2\pi/l_0$ that defines the Kolmogorov spectrum to the range O to ∞adds a small contribut ion. For $K << 2\pi/L_0$, the integrand in eqn. [3.9] is bounded for all z and goes to zero as $K^{4/3}$ for small K. Thus the contribution to the integral is vanishingly small for $0 < K < 2\pi/L_0$. This is consistent with the expectation that the outer scale of turbulence contributes only to beam wander and not to stint illation. For $K >> 2\pi/l_0$, where l_0 is on the order of millimeters, spatial frequencies arc approximately 103 m^{-1} and the integrand decays as $K^{-8/3}$ so that the contribution from extending the integral beyond $2\pi/l_0$ is again vanishingly small. integrating over K wc get

$$\sigma_\chi^2 = 4\pi^2(0.033)k^2 \left[\frac{\pi}{\sqrt[3]{4(1+\sqrt{3})}\,\Gamma(\frac{11}{6})}\right] \int_0^L C_n^2(z) \left(\frac{5/6}{}\right) \frac{(L-z)^{5/6}}{(2kz)^{5/6}} dz$$

$$= 0.56k^{7/6} \int_0^L C_n^2(z)(z/L)^{5/6}(L-z)^{5/6} dz. \qquad 3.10$$

in our experiment the terrain falls off rapidly at both the transmitter and receiver sites with most of the propagation path high above the valley floor. Wc therefore considered C_n^2 a constant along the path, and took it outside the integral in eqn. [3.10]. The integral thus reduces to the Beta function B(r,s) and the log-amplit udc variance is given by

$$\sigma_\chi^2 = C_n^2 k^{7/6} L^{11/6} B(\tfrac{11}{6}, \tfrac{11}{6})$$

$$= 0.124\text{C:k7'61:1'6}. \qquad 3.11$$

The log-amplitude variances calculated from the measured irradiance variances were used with eqn. [3.11] to calculate C_n^2 for the three experiment runs. These results arc listed in I'able 1 along with the value of C_n^2 calculated for a 2 km altitude using the AFGL CLEAR 1 Night Model[6] for comparison. Our results show good agreement with this model.

3.3 Aperture Averaging

Irradiance variations, (fades and surges in the received signal) can cause errors in the communications channel and degrade the performance of the link. However these random fluctuations can be averaged out by increasing the size of the receiving aperture. The aperture averaging factor "A", is defined as the ratio of the intensity variance for an aperture "D" to that for a point detector; $A = (\sigma^2_I(D)/\sigma^2_I(0))$. Wc follow the development of Fried[7] and Churnside[8] where "A" for a circular aperture D has been given by:

$$A = \frac{16}{\pi D^2}\int_0^D \frac{C_I(\rho)}{C_I(0)}\left[\cos^{-1}\left(\frac{\rho}{D}\right) - \frac{\rho}{D}\left\{1 - \left(\frac{\rho}{D}\right)^2\right\}^{1/2}\right]\rho d\rho \qquad 3.12$$

Where $C_I(\rho)$ is the covariance function of the irradiance for two apertures whose centers are displaced by a distance ρ. For spherical wave propagating $C_I(\rho)$ is given by

$$C_I(\rho) = (0.033)1.6\pi^2 k^2 C_n^2 \int_0^\infty K^{-8/3} dK \int_0^L \sin^2\left\{\frac{K^2(L-z)z}{2kL}\right\} J_0\left(K\rho\frac{z}{L}\right) dz \qquad 3.13$$

for a Kolmogorov spectrum, and

$$C_I(0) = (0.033)1.6\pi^2 k^2 C_n^2 \int_0^\infty K^{-8/3} dK \int_0^L \sin^2\left\{\frac{K^2(L-z)z}{2kL}\right\} dz \qquad 3.14$$

The aperture averaging factor is then given by[8]

$$A = 53.4 k^{5/6} L^{-11/6} \int_0^\infty K^{-8/3} dK \int_0^L \sin^2\left\{\frac{K^2(L-z)z}{2kL}\right\} dz \int_0^1 \left[\cos^{-1}(s) - s\left\{1 - (s)^2\right\}^{1/2}\right] J_0\left(KsD\frac{z}{L}\right) ds \qquad 3.15$$

Where $J_0(Ksz/D)$ is the zeroth order Bessel function.

Numerical integration of eqn. [3. 15] for different values of D gives the aperture averaging factor as a function of diameter.[8] This integration was not done. Instead we used Churnside's[8] approximation to bound A. See figure 5. This approximation is given by

$$A = [1 + 0.214(\frac{k D^2}{4L})^{7/6}]^{-1} \qquad 3.16$$

We have measured "A", at midnight, 4:00 A. M., and 6:00 A.M. and the data sets throughout the night showed a consistent pattern decreasing from 0.7 at the 4 cm aperture to 7x10-2 for the 28.7 cm aperture. These results are shown in figure 5 where the measured A is plotted as a function of the Fresnel number.

3.4 Bit Error Rate measurement

For a Gaussian white noise channel the bit-error-rate for non coherent detection is given by[9]

$$BER = 0.5e^{-0.5SNR} \qquad 3.17$$

Where we have assumed a Gaussian white noise channel.

Yura [10] has shown that the degradation in SNR due to turbulence can be written as

$$\frac{SNR}{SNR_o} = \frac{1}{(1 + A\sigma_{\ln I}^2)} \qquad 3.18$$

Where SNR_0 is the signal-to-noise ratio in the absence of turbulence, A is the aperture averaging factor and $\sigma^2_{\ln I}$ is the log-intensity variance. The BER is thus given by:

$$BER = 0.5e^{\frac{SNR_o}{2(1+A\sigma_{\ln I}^2)}} \qquad 3.19$$

Bit error rate measurements were made as described in Section 2. The BERT sampled the data for one second and generated an error whenever the output signal deviated from the expected pattern. Ten to fifteen measurements were made over about a 20 second interval, and the BER were recorded and averaged over the interval for each selected aperture diameter.

Table 2 gives the results for the midnight experiment run. The dramatic increase in the measured BER with decreasing aperture size shown in Table 2 is due to the reduction in signal power with decreasing apertures, and not the result of turbulence. The estimated reduction in SNR due to turbulence for the apertures of 28.7, 21.7 and 15.4 cm effective diameter is only 1 %, 3% and 15%, respectively. However, there is a 2.5 dB decrease in signal as the aperture is reduced

from *28.7 cm* to *21.7* cm and an additional 2.7 dB as the aperture is further reduced to 15.4 cm. We have used eqn. [3. 17] to predict the BERs corresponding to these signal levels. These arc also given in Table 2.

4. CONCL1JS1ONS

We have measured the effects of atmospheric turbulence on opt ical communicant ions across a 42 km long horizontal path. The measurements were conducted at night when turbulence is low. The results clearly showed a log-normal distribution of the log irradiance for the larger apertures. The normalized irradiance variance, hence "A" decreased by an order of magnitude as the collecting aperture increased from 4 cm to *28.7 cm.* This decrease is much more rapid than predicted by the Churnside approximation. This discrepancy is first duc to the approximation. Churnside's comparison of his approximation with the exact numerical solution shows that the approximation is about a factor of 2 too large. Second, wc believe that since our log-amplitude variances indicate that our turbulence conditions were C1OSC to saturation, mixing among turbulent eddies effectively aperture averaged the scintillation effects.

S. ACKNOWLEDGMENTS

We acknowledge J. Lcsh Supervisor JPL Optical Communications Group for his critical reading of this manuscript and for his support throughout the experiment. Wc also acknowledge C. S. Liu of Thermo Trex Corporation, and S. Gil lam and J. Young of the Table Mountain Facility. The authors give a special word of thanks to A. Harris and I. Chen of Thermo Trex Corporation for their dedication in establishing and maintaining the link from Strawberry Peak.

The work described in this paper was performed and by the Jet Propulsion Laboratory, California Institute of Technology, under contract with the National Aeronautics and Space Administrat ion It was also supported by the Thermo Trex Corporation under contract to the Ballistic Missile Defense Organization.

6. REFERENCES

1. M. E. Gracheva, A. S. Gurvich, and M. A. Kallistratova, "Measurement of the Average Amplitude of a Light Wave propagating in a Turbulent Atmosphere," Izvestiya VUZ. Radiofizika, vol. 13, no. 1, pp. 50-55, 1970 (translation)
2. A. Ishimaru Wave Propagation and Scattering in Random Media vol. 2. (Academic Press New York, 1978) pp. 349 -352.
3. A. Ishimaru Wave Propagation and Scattering in Random Media vol. 2. (Academic Press, Ncw York, 1978) pg. 367.
4. The Infrared Electro-optical systems Handbook, vol. 2 Atmospheric Propagation of Radiation. F. Smith, Editor, SPIE Optical Engineering Press, Washington (1993) pp. 220.
5. A. Ishimaru Wave Propagation and Scattering in Random Media vol. 2. (Academic Press, Ncw York, 1978) pg. 385.
6. The Infrared Handbook revised edition, W. Wolfe and G. Zissis Editors Environmental Research Institute of Michigan, (1989) pg. 6-18.
7. D. L. Fried, "Aperture Averaging of Scintillation," J. Opt. Sot. Am., vol. 57, no. 2, pp. 169 - 17S, 1967.
8. J. Churnside, " Aperture Averaging of Optical Scintillations in the Turbulent Atmosphere", Applied Optics, vol. 30, no. 15, pp. 1982-1994, 1991.
9. S. Haykin, Communications Systems Third edition (John Wiley & Sons inc., Ncw York, 1994) pp. 532-540.
10. H. Yura, "Ef'feels of At mospheric Turbulence on Optical Communicat ions from Space to Ground" Aerospace Report no. ATR-94(6486)-5, April 1993, pg. 1.

Table 1

Normalized irradiance variances for the various aperture sires calculated from measured irradiance fluctuations at the three experiment runs. Also shown arc the corresponding calculated log-amplitude variances and C_n^2 values.

Effective aperture diameter, cm	Fresnel number		Normalized Irradiance Variance	
		12:00	4:00 A. M.	6:00 A.M.
28.7	1.93	0.139	0.28	0.155
21.7	1.46	0.254	0.441	0.213
15.4	1.03	0.695		
9.33	0.662	0.77		
7.02	0.471	1.08	1,72	0.576
4.08	0.274	1.43	2.43	1.44
σ^2_x		0.28	0.37	0.27
Cn^2	Calculated from data	7.22E-17	9.26E-17	6.96E-17
	AFGL CLEAR 1 night Model	4.6E-17		

Table 2

Bit error rates, BER, measured for the three largest aperture sires during the midnight experimental run. These arc compared with the BER* determined from the expected reduction in SNR with decreasing aperture size.

Effective aperture diameter, m	BER	BER*
28.7	$2.48E^{-6}$ ($+5.27E^{-6}$ $-2.48E^{-6}$)+	-
21.7	$3.54E^{-5}$ (+/-$6.27E^{-6}$)	$0.75E^{-5}$
15.4	$1.58E^{-2}$ (+/-$8.38E^{-3}$)	$1.52E^{-2}$

'The large standard deviation in this data reflects the bursty channel in which measured BERs ranged from a high of 10^{-5} to a low of 10^{-9} over the measurement interval.

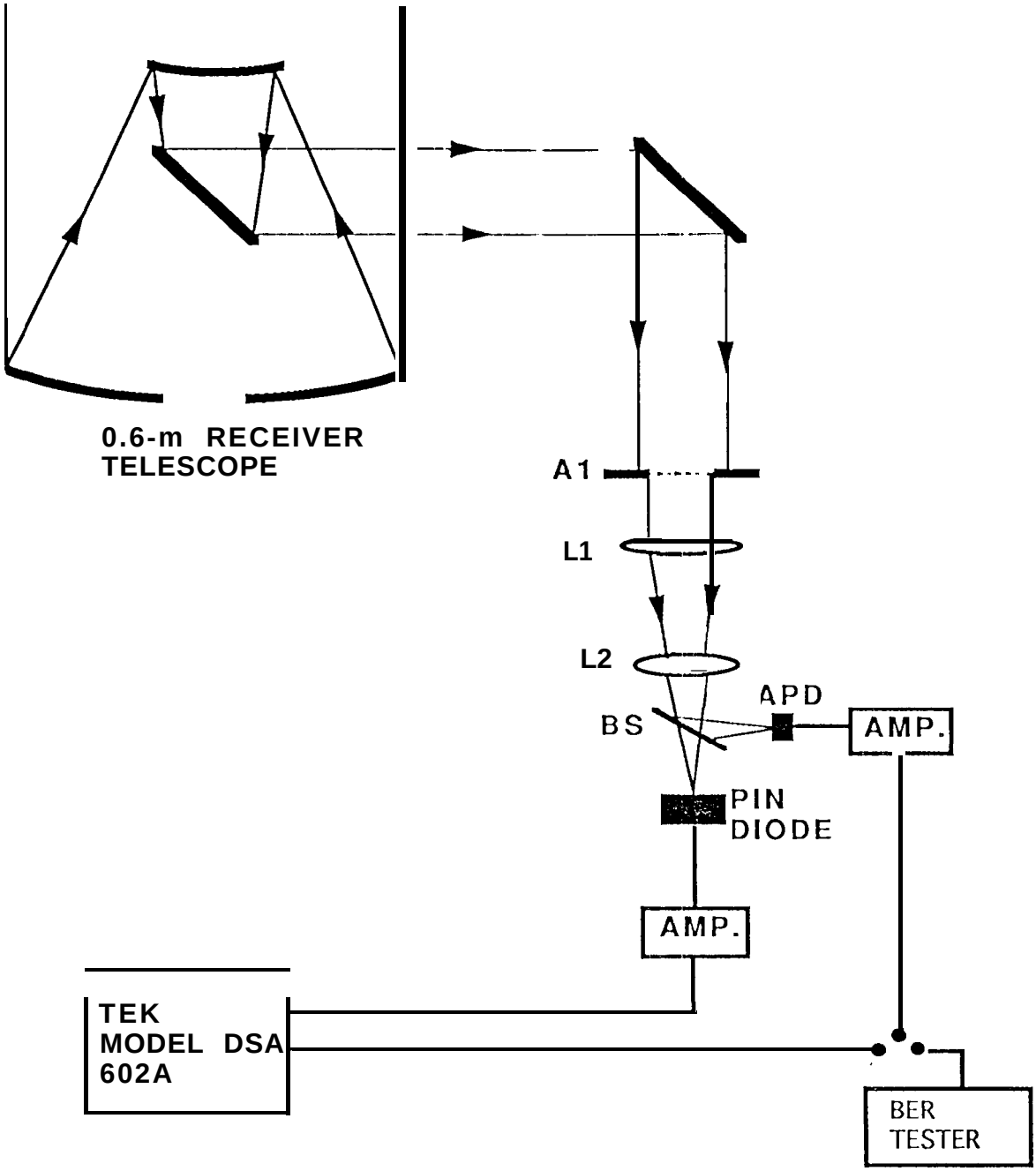

Figure 1: Schematic showing receiving telescope Optics and receiver electronics. the variable aperture A1 wasused to adjust the effective receiving diameter of the telescope. Lenses L1 and L2 focused the received laser beam through the 40°A reflectivity beamsplitter (BS) and on to the high speed APD that was used **to measure** the bit error rate. the lower bandwidth pin diode was used to measure the turbulence induced irradiance fades.

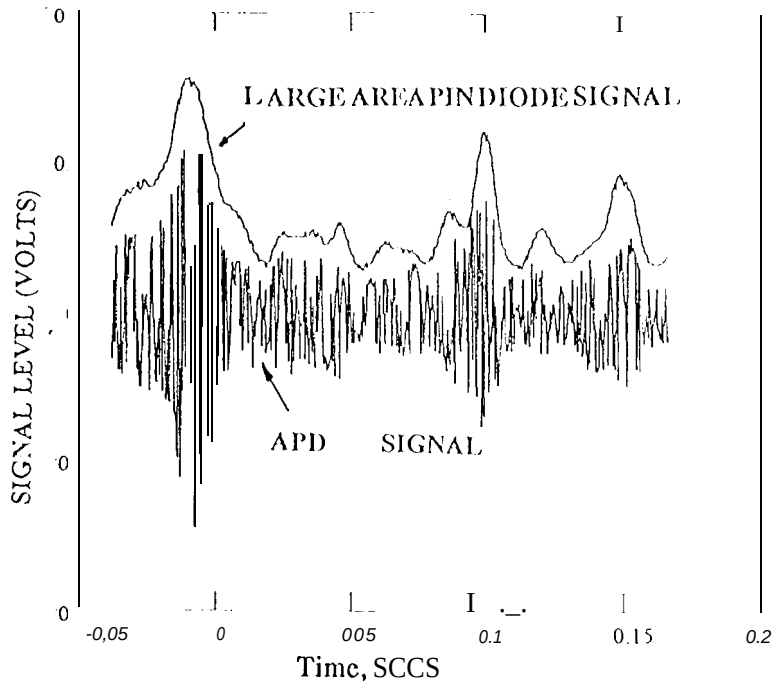

Figure 2: Traces from high speed communications detector (APD) and low bandwidth UDT photodiode showing modulation of communications signal intensity by atmospheric turbulence.

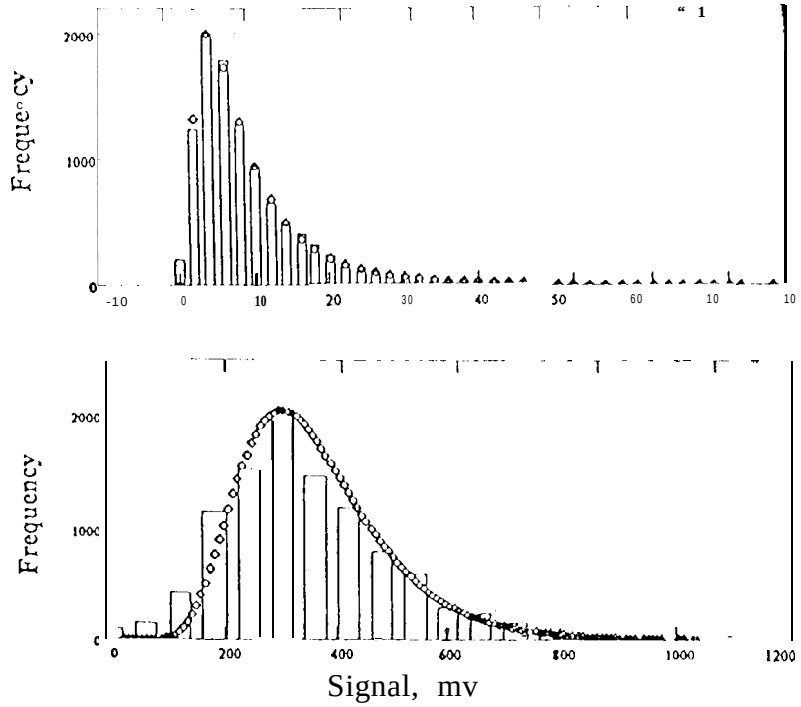

Figure 3: Histogram showing typical measured and fitted log-intensity fluctuations for 4 cm (upper plot) and 28 cm (lower plot) apertures. The data are shown for the 12:00 A.M. run, The measured (Table 1) and fitted variances are 0.89, 0.56 for the 4 cm aperture and 0.14, 0.14 for the 28 cm aperture.

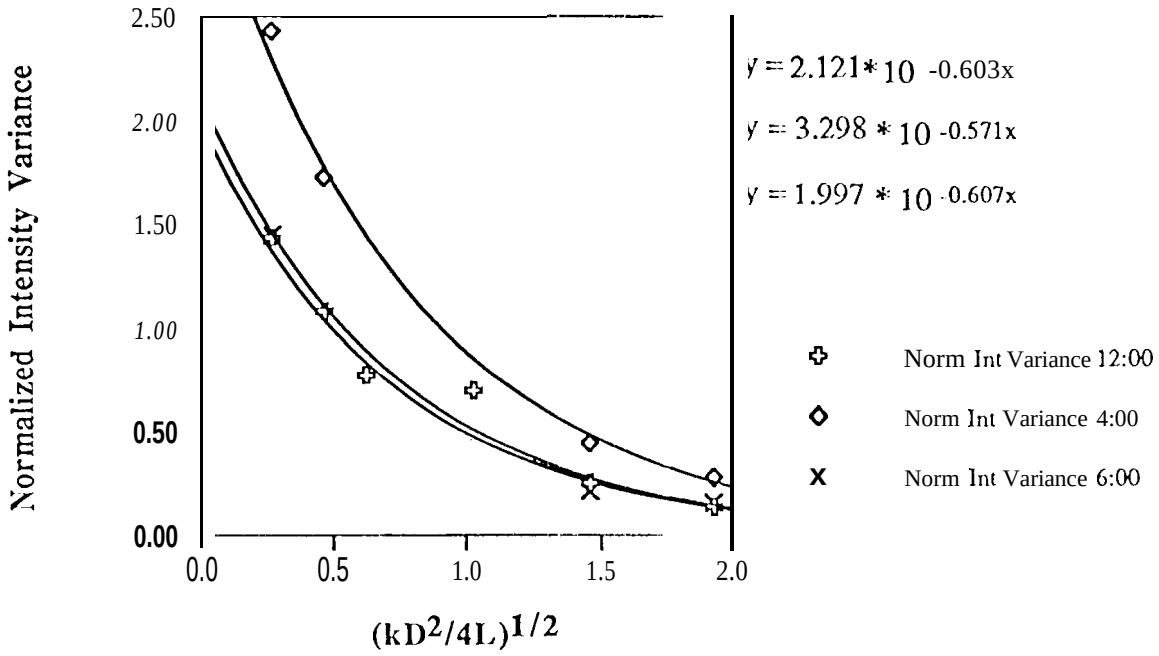

Figure 4: Plot of normalized intensity variance vs. Fresnel number for t he thi cc experimental runs, The y intercept of the curves was used to determine the log-amplitude variance.

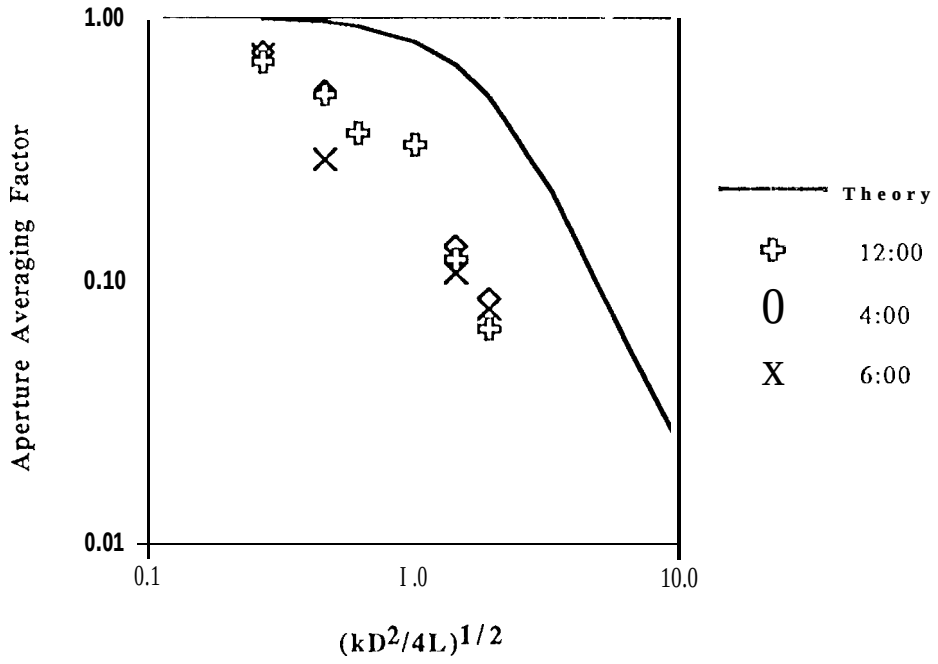

Figure 5. Aperture averaging factor vs Fresnel number for the three experimental runs. The aperture averaging factor calculated for a spherical wave using the Churnside approximation for large D is shown for reference.